Applied Thermal Engineering 256 (2024) 124053

Contents lists available at ScienceDirect

Applied Thermal Engineering

journal homepage: www.elsevier.com/locate/apthermeng

Research Paper

Recovered water from fuel cells as a supply for Maisotsenko evaporative cooling systems in a hydrogen-powered urban bus

Marco Puglia [a], Nicolò Morselli [a], Michele Cossu [a], Simone Pedrazzi [a,b], Giulio Allesina [a,b], Alberto Muscio [a,b,*]

[a] Dipartimento di ingegneria "Enzo Ferrari", Università degli Studi di Modena e Reggio Emilia, Via Vivarelli 10/1, 41125 Modena, Italy
[b] INTERMECH, Dipartimento di ingegneria "Enzo Ferrari", Università degli Studi di Modena e Reggio Emilia, Via Vivarelli 10/1, 41125 Modena, Italy

A B S T R A C T

The EU ban on the sale of new petrol and diesel cars from 2035 requires finding sustainable alternatives both from an energy and an environmental point of view. The path now seems to be drawn towards a total electrification of public and private transportation sectors. However, the issue of the limited range of electric vehicles, particularly for heavy-duty ones, still needs to be addressed. The development of fuel cell vehicles powered by compressed hydrogen, not relying exclusively on batteries, can achieve ranges comparable to those powered by fossil-fuel. The development of hydrogen vehicles must proceed in parallel with increasing the efficiency of passenger compartment air conditioning, which requires a significant share of the total energy consumed. An efficient alternative to common vapor compression cooling systems is represented by evaporative coolers, in which water evaporation is used to cool an air flow. This study investigates the feasibility of utilizing the recovered water from the exhaust gas of a hydrogen PEM fuel cell, powering an urban bus, within a commercial indirect evaporative cooling system employing the Maisotsenko cycle. The cooling capacity of the proposed system was calculated to verify the possibility of implementing it on an urban bus. The water available at the cathode of the fuel cell and the water required by the evaporative cooler were evaluated under various conditions and compared. The calculations demonstrate that even under intense weather conditions, where approximately 40 kg of water may be required every hour, at least 10 % of water needed by the evaporative cooling system can be provided by the water produced through the hydrogen reaction. In mild weather conditions or by cooling the exhaust, it is possible to significantly increase the share of pure water supplied to the evaporative system. The integration of hydrogen fuel cells and evaporative coolers in bus equipment can be an energy-efficient, win–win solution. This configuration enables the dual utilization of the hydrogen employed to drive the fuel cell.

1. Introduction

The reduction of greenhouse gases and pollutant emissions is pushing the transport sector to increase the use of energy-efficient and alternative powertrains. The European Union is moving to ban gasoline and diesel engine sales for private transportation with the goal of reaching a complete substitution of powertrains fueled with fossil fuels [16]. In this context, public transportation is also going to be affected by this shift. In fact, public transport represents a significant share of the production of noise emissions and harmful gases at urban level [18] and the plan for the development of an all-electric city bus network can be dated back to 2014. To date, most electric buses are powered by onboard batteries. However, the limitation of this technology lies in the short driving range and long recharging time which limit its large-scale diffusion [26]. A possible alternative is represented by hydrogen fuel cells that can be a crucial actor in the decarbonization of vehicles [14,2]. The fuel cell is an electrochemical device where the chemical energy of a carrier (often hydrogen) is converted into electric energy by means of reduction oxidation reaction [10,11]. Among the various technologies, the proton exchange membrane fuel cell (PEMFC) is the most promising due to its low operating temperature (60–80 °C), low noise, quick start-up and high-power density, making its suitable for automotive industry but also for aircraft and spacecraft [6,17,23,24,42]. The overall chemical reaction occurring in a PEMFC can be summarized as $H_2 + \frac{1}{2}O_2 \rightarrow H_2O$ [20,41]. However, up to today, fuel cell vehicles are not as competitive as battery electric vehicles in terms of technology readiness levels, costs and limited infrastructure. However, hydrogen can be extremely interesting when high load capacity and long driving range are required [14]. In fact, the longer driving distances and the short refueling times make heavy-duty vehicles powered by hydrogen competitive compared to full electric ones [25,51]. In particular, fuel cell electric buses are a quite established technology, as shown by the various public transport hydrogen-powered fleets in several locations worldwide [25]. The range is often hindered by energy consumption that goes beyond the vehicle's traction alone, such as consumption related to the summer air conditioning of the passenger compartment [27]. Approximately 6 % of the energy consumed by cars globally is due to mobile air conditioning, and

* Corresponding author.
E-mail address: alberto.muscio@unimore.it (A. Muscio).

https://doi.org/10.1016/j.applthermaleng.2024.124053
Received 27 December 2023; Received in revised form 24 July 2024; Accepted 26 July 2024
Available online 28 July 2024

Nomenclature

c	*Specific heat capacity* ($\frac{J}{kgK}$)
CC	*Cooling capacity (W)*
c_p	*Specific heat capacity at constant pressure* ($\frac{J}{kgK}$)
h_{lv}	*Latent heat of vaporization* ($\frac{J}{kg}$)
m	*Mass (kg)*
$\dot{m}$	*Mass flow rate (kg/s)*
M	*Molar mass* ($\frac{g}{mol}$)
n	*Number of moles (mol)*
p	*Pressure (Pa)*
R	*Universal gas constant* ($\frac{J}{kmolK}$)
r_V	*Supply to inlet volume flow ratio (−)*
r_m	*Supply to inlet mass flow ratio (−)*
T	*Temperature (K)*
V	*Volume* (m^3)
$\dot{V}$	*Volume flow rate* (m^3/s)

Greek letters

φ	*Relative humidity (−)*
ρ	*Density* ($\frac{kg}{m^3}$)
ε	*Effectiveness (−)*

Subscripts

i	*i-th component*
da	*Dry air mixture*
sat	*Vapor saturation condition*
l	*Liquid state*
v	*Vapor state*
amb	*External environment*
$cabin$	*Internal environment*
FC	*Fuel cell*
in	*Fuel cell inlet duct*
out	*Fuel cell outlet duct*
inj	*Injected*
$prod$	*Produced in the reaction*
req	*Required for the reaction*
$cool$	post-cooling conditions
di	*Dry channel inlet*
do	*Dry channel outlet*
wo	*Wet channel outlet*
DP	*Dew point*
rec	*Recovered water for the M-cycle*

in hot climates and intense traffic conditions, this can peak at significantly higher values [40]. For an urban bus, the power spent on the summer air conditioning system is in the range of 20 % of the average power supplied by the powertrain for travel [29,7]. In fact, the most widespread air conditioning systems rely on the use of vapor compression recirculation systems (VCRs) which often work with COP (coefficient of performance) lower than 3, greatly limiting the efficiency of this solution [45]. Current methodologies of thermal management for electric vehicles derive from solutions applied to internal combustion engine vehicles. However, this solution is more challenging when considering medium-duty vehicles compared to cars due to differences in driving scenarios [39]. An alternative to VCRs is represented by indirect evaporative cooling cycles (IEC) in which the latent heat of evaporation of the water is used to extract energy from an air flow [13]. To the best of the authors' knowledge, there are no precedent studies regarding the use of indirect evaporative cooling systems for the air conditioning of a bus. [44] presented a research on the application of a direct evaporative cooling (DEC) system on an urban bus. However, unlike DECs, IECs present a physical separation between the wet side and the dry side of the heat exchanger, preventing excessively humid air from being sent to the end user [4,5]: in this case, the cabin of a bus. To obtain the best performance with an evaporative cooling system, it is necessary to increase air change rates without recirculation [46]. This peculiarity of IECs makes them extremely interesting for crowded places like urban buses, as high air changes per hour can be a key factor in reducing the infection risk in the presence of respiratory pathogens [47,48]. Among the IECs, the Maisotsenko's cycle (M−cycle) is the most promising, guaranteeing coefficients of performance (COP) far superior to the vapor-compression refrigeration (VCR) cycle, normally reaching values between 5 and 20 as reported by Zhu et al. and by Dizaji et al., [28,30]. The M−Cycle is a thermodynamic process that, unlike traditional direct and indirect evaporative cooling systems, can potentially cool the air down to the dew point temperature rather than the wet bulb temperature [43]. Additionally, aside from producing cooled air, the M−Cycle also generates saturated air as a byproduct, which can be useful in various applications. The heat and mass exchanger used for the M−cycle, as depicted in Fig. 1A, is composed of two types of channels: wet channels and dry channels. In the dry channels, the primary flow passes releasing heat, while in the wet channels, the water is injected to evaporate and absorb the heat from the dry channels. The same air flow passes through both channels. Towards the end of the dry channel in the heat and mass exchanger, a portion of the air is diverted into the wet

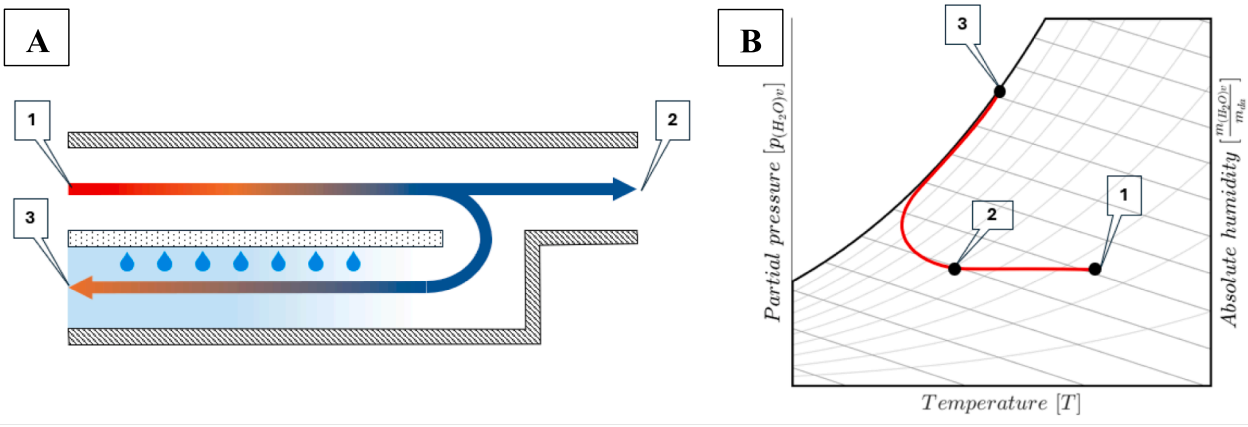

Fig. 1. Schematic representation (A) and psychrometric chart representation (B) of the M−cycle process.

channel to serve as the working fluid. In the wet channel, the air is humidified through water evaporation. This process enables the conversion of sensible heat in the dry channel into latent heat of evaporation absorbed by the wet channel [30]. Furthermore, the air introduced into the working channel at the end of the sensible heat transfer in the primary channel enters in a pre-cooled state [37], as illustrated in the psychrometric chart (Fig. 1B).

The objective of this study is to evaluate the recovery and reuse of water from the exhaust of a hydrogen fuel cell in the Maisotsenko evaporative cooling system of a bus, aiming to reduce the system's pure water consumption. The cooling capacity was calculated using a Seeley tool, specifically referring to the CW-*H*10 Indirect Evaporative Cooler manufactured by Seeley International [32]. Seeley International is a leading manufacturer of evaporative cooling systems. The recoverable water at the fuel cell exhaust was calculated using psychrometric equations. Water consumption of the considered evaporative cooling system and quantity of water recovered from the fuel cell were subsequently compared. Having an onboard water recovery system capable of extracting water from the exhaust gas can be extremely useful, regardless of the presence of an evaporative cooling system. This is because the water recovered from the outlet can be utilized to maintain the proper membrane humidity, which is a crucial parameter for ensuring the optimal operation of a PEM fuel cell [12].

2. Materials and methods

This section begins by describing the calculation of the operating stoichiometry of the fuel cell, which leads to the determination of the amount of liquid water produced per unit of hydrogen consumed. Subsequently, the section explains the calculation used to analyze the indirect evaporative cooler based on the Maisotsenko cycle. Here, the performance of the M−cycle is evaluated through the tool provided by Seeley International which, based on the inlet conditions, provides the outlet temperature from the dry channel of the heat and mass exchanger. The results of the two models are compared to evaluate the feasibility of recovering water from the fuel cell of a hydrogen-powered urban bus for use as a supply for its M−cycle based air conditioning unit.

2.1. Inlet air mixture

Atmospheric air is a mixture of gases composed primarily of diatomic oxygen, diatomic nitrogen, and water vapor. The definition of dry mixture refers to the composition of the mixture of gases in the air excluding water vapor, while the term wet mixture refers to the complete mixture that includes water vapor. To a first approximation, these gases can be treated as perfect gases, and the mixture itself can be considered a perfect gas. For the psychrometric calculations it is necessary to calculate the equivalent molar mass of the perfect gas mixture. In this work the dry air mixture was considered to be composed of oxygen (O_2), nitrogen (N_2) and Argon (Ar) with volume fractions of 21 %, 78 % and 1 % respectively [35]. At the cathode of a fuel cell, a fraction of oxygen participates in the electrochemical reaction and is consumed. As a result, the composition of the exhaust dry mixture is different from that in the inlet duct. To analyze this system, it is necessary to distinguish between the molar mass and the mass flow upstream and downstream of the electrochemical cell. For the mixture of dry gases upstream of the cell, the molar mass $M_{da,amb}\left[\frac{g_{da}}{mol_{da}}\right]$ can be calculated using the formula:

$$M_{da,amb} = \sum_{i,amb} \frac{V_{i,amb}}{V_{da,amb}} M_{i,amb} \left[\frac{g}{mol}\right] \tag{2.1}$$

where the index i indicates the i-th component of the gas mixture. The mass fraction of the individual gases compared to the dry mixture, starting from their volume fraction within the same dry mixture, is obtained through the relation:

$$\frac{m_{i,amb}}{m_{da,amb}} = \frac{V_{i,amb}}{V_{da,amb}} \frac{M_i}{M_{da,amb}} \left[\frac{kg_i}{kg_{da}}\right] \tag{2.2}$$

2.2. Stoichiometric air calculation

Knowing the mass of oxygen required in relation to the mass of reacted hydrogen, it is possible to calculate the stoichiometric mass of dry air $m_{da,req,in}$ to be flowed inside the fuel cell for each mass unit of hydrogen that took part in the reaction m_{H_2}. In fact, this dry air will contain the quantity of oxygen necessary for the reaction $m_{O_2,req}$.

$$\frac{m_{da,req,in}}{m_{H_2}} = \frac{\frac{m_{O_2,req}}{m_{H_2}}}{\frac{m_{O_2}}{m_{da,amb}}} \left[\frac{kg_{O_2}}{kg_{H_2}}\right] \tag{2.3}$$

The calculation of the mass of oxygen required $m_{O_2,req}$ and the mass of produced water $m_{H_2O,prod}$ in relation to the mass of reacted hydrogen m_{H_2} is provided in the Appendix A.

2.3. Air flow calculation

Relationship 2.3 should be updated with the excess ratio coefficient to calculate the mass of inlet dry air per mass unit of hydrogen that takes part in the reaction. Excess ratio λ is the ratio between the oxygen inlet mass flow rate and the oxygen mass flow that actually reacts in the fuel cell. In fact, not all the oxygen that flows in the pipeline takes part in the electrochemical reaction and therefore an excess amount of oxygen is necessary [33]. With the hypothesis of perfect mixing of the components it can be stated that the excess air coefficient can be used for each component of the mixture and it can also be used to consider the ratio of the total mass of dry air flowed $m_{da,in}$ and the stoichiometric mass of dry air required $m_{da,req,in}$. Therefore, the mass of dry air $m_{da,amb}$ to be flowed inside the fuel cell for each mass unit of hydrogen that took part in the reaction m_{H_2} becomes:

$$\frac{m_{da,amb}}{m_{H_2}} = \frac{\lambda \frac{m_{O_2,req}}{m_{H_2}}}{\frac{m_{O_2}}{m_{da,amb}}} \left[\frac{kg_{da}}{kg_{H_2}}\right] \tag{2.4}$$

2.4. Inlet water injection

The membrane of a PEM fuel cell needs to be kept constantly hydrated to offer maximum performance [12], for this reason it is necessary to ensure that inside the cell there is an air flow in a near saturation condition [38]. The saturation pressure at the temperature of the cell $T_{FC,in}$ can be estimated from the following relationship [34]:

$$p_{(H_2O)v,sat,FCin} = 610.5 e^{\frac{17.269 T_{FCin}}{237.3 + T_{FCin}}} [Pa] \tag{2.5}$$

By imposing the desired relative humidity inside the cell φ_{FCin}, the vapor pressure at the inlet section of the fuel cell is calculated:

$$p_{(H_2O)v,FCin} = \varphi_{FCin} p_{(H_2O)v,sat,FCin} [Pa] \tag{2.6}$$

From this, the absolute humidity at the fuel cell cathode inlet is calculated as:

$$\frac{m_{(H_2O)v,FCin}}{m_{da,in}} = \frac{M_{H_2O}}{M_{da,in}} \frac{p_{(H_2O)v,FCin}}{p_{FCin} - p_{(H_2O)v,FCin}} \left[\frac{kg_{H_2O}}{kg_{da}}\right] \tag{2.7}$$

In this work the ambient pressure was considered 101325Pa while different operating pressures were considered for the cathode. At the cell entrance, the composition of the dry gas mixture has not changed compared to the initial condition, therefore the amount of water needed per mass unit of reacted hydrogen can be calculated by multiplying the absolute humidity by the mass of dry air entering per mass unit of

reacted hydrogen calculated with 2.4:

$$\frac{m_{(H_2O)v,FCin}}{m_{H_2}} = \frac{m_{(H_2O)v,FCin}}{m_{da,amb}} \frac{m_{da,amb}}{m_{H_2}} \left[\frac{kg_{H_2O}}{kg_{H_2}}\right] \tag{2.8}$$

The water that needs to be added inside the inlet duct to increase the flow humidity from the ambient value to the desired one is obtained by difference:

$$\frac{m_{H_2O,inj}}{m_{H_2}} = \frac{m_{(H_2O)v,FCin}}{m_{H_2}} - \frac{m_{(H_2O)v,amb}}{m_{H_2}} \left[\frac{kg_{H_2O}}{kg_{H_2}}\right] \tag{2.9}$$

The calculation of the mass of incoming water vapor from the ambient $m_{(H_2O)v,amb}$ per mass unit of reacted hydrogen is provided in the Appendix B.

2.5. Exhaust gas composition

As already analyzed, at the cell exhaust there is a gas mixture composed of the excess unreacted oxygen, nitrogen, other inert gases (mostly argon) and water. The quantity of water at the exhaust is equal to the sum of the atmospheric one, the water injected at the fuel cell inlet and the water generated as a product of the electrochemical reaction. The water downstream of the cell can be in both vapor and liquid form. The quantity of oxygen in the mixture of dry gases at the outlet of the cell has decreased. The mass and molar mass of the dry mixture of the exhaust are therefore different from the corresponding values in the inlet pipe. The molar mass of the dry gas mixture at the exhaust $M_{da,out}$ can be calculated starting from the definition:

$$M_{da,out} = \frac{m_{da,out}}{n_{da,out}} \left[\frac{g}{mol}\right] \tag{2.10}$$

Where $m_{da,out}$ is the mass of dry mixture at the exhaust:

$$m_{da,out} = \sum_{i,out} m_{i,out}[kg] \tag{2.11}$$

from which:

$$M_{da,out} = \frac{\sum_{i,out} m_{i,out}}{n_{da,out}} = \sum_{i,out} \frac{m_{i,out}}{n_{da,out}} \left[\frac{g}{mol}\right] \tag{2.12}$$

By substituting the mass of the individual components of the mixture with their number of moles multiplied by their corresponding molar mass, we obtain:

$$M_{da,out} = \sum_{i,out} \frac{n_{i,out} M_{i,out}}{n_{da,out}} \left[\frac{g}{mol}\right] \tag{2.13}$$

This relationship can be calculated by considering the mole fractions of the gases with respect to the moles of hydrogen:

$$M_{da,out} = \sum_{i,out} \frac{\frac{n_{i,out}}{n_{H_2}}}{\frac{n_{da,out}}{n_{H_2}}} M_{i,out} \left[\frac{g}{mol}\right] \tag{2.14}$$

The mole fraction of oxygen at the cell outlet with respect to the moles of hydrogen is equal to the mole fraction of the incoming oxygen minus the mole fraction of oxygen reacted with hydrogen. The moles of incoming oxygen are the stoichiometric moles multiplied by the excess ratio coefficient:

$$\frac{n_{O_2,out}}{n_{H_2}} = \frac{n_{O_2,in}}{n_{H_2}} - \frac{n_{O_2,req}}{n_{H_2}} = \lambda \frac{n_{O_2,req}}{n_{H_2}} - \frac{n_{O_2,req}}{n_{H_2}} = (\lambda - 1) \frac{n_{O_2,req}}{n_{H_2}} \left[\frac{mol_{O_2}}{mol_{H_2}}\right] \tag{2.15}$$

The amount of the inert gases at the outlet and at the inlet are equal. The mole fraction of the inert gases in relation to the moles of hydrogen can be calculated from the mass fraction with respect to hydrogen. As done for oxygen, the mass fraction of a gas in the mixture related to the reacted hydrogen is calculated from the relations 2.2 and 2.4.

$$\frac{m_{i,out}}{m_{H_2}} = \frac{m_{i,in}}{m_{H_2}} = \frac{m_{i,in}}{m_{da,amb}} \frac{m_{da,amb}}{m_{H_2}} \left[\frac{kg_i}{kg_{H_2}}\right] \tag{2.16}$$

As an example, the calculation of the moles of nitrogen in the exhaust becomes:

$$\frac{n_{N_2,out}}{n_{H_2}} = \frac{n_{N_2,in}}{n_{H_2}} = \frac{\frac{m_{N_2,in}}{M_{N_2}}}{\frac{m_{H_2}}{M_{H_2}}} = \frac{m_{N_2,in}}{m_{H_2}} \frac{M_{H_2}}{M_{N_2}} \left[\frac{mol_{N_2}}{mol_{H_2}}\right] \tag{2.17}$$

The mole fraction of the dry mixture in relation to the moles of hydrogen is therefore the sum of the mole fractions of the gases that compose it:

$$\frac{n_{da,out}}{n_{H_2}} = \sum_{i,out} \frac{n_{i,out}}{n_{H_2}} \left[\frac{mol_{da}}{mol_{H_2}}\right] \tag{2.18}$$

At this point it is possible to calculate the molar mass of the dry mixture at the exhaust $M_{da,out}$. The absolute saturation humidity in the outlet section of the cell is calculated by referring to the mixture of dry gases at the exhaust $m_{d,out}$.

$$\frac{m_{(H_2O)v,FCout}}{m_{da,out}} = \frac{m_{(H_2O)v,sat,FCout}}{m_{da,out}} = \frac{M_{H_2O}}{M_{da,out}} \frac{p_{(H_2O)v,sat}(T_{FCout})}{p_{FCout} - p_{(H_2O)v,sat}(T_{FCout})} \left[\frac{kg_{H_2O}}{kg_{da}}\right] \tag{2.19}$$

The ratio between the mass of dry gases at the exhaust compared to the mass of reacted hydrogen is calculated as a function of the mole fraction of the dry mixture compared to hydrogen.

$$\frac{m_{da,out}}{m_{H_2}} = \frac{n_{da,out}}{n_{H_2}} \frac{M_{da,out}}{M_{H_2}} \left[\frac{kg_{da}}{kg_{H_2}}\right] \tag{2.20}$$

The mass fraction of vapor in saturated condition referred to the mass of reacted hydrogen is then obtained.

$$\frac{m_{(H_2O)v,FCout}}{m_{H_2}} = \frac{m_{(H_2O)v,FCout}}{m_{da,out}} \frac{m_{da,out}}{m_{H_2}} \left[\frac{kg_{H_2O}}{kg_{H_2}}\right] \tag{2.21}$$

The mass fraction of water at the outlet is the sum of the water at the inlet section plus the water produced during the electrochemical reaction.

$$\frac{m_{H_2O,FCout}}{m_{H_2}} = \frac{m_{H_2O,FCin}}{m_{H_2}} + \frac{m_{H_2O,prod}}{m_{H_2}} \left[\frac{kg_{H_2O}}{kg_{H_2}}\right] \tag{2.22}$$

It is evident from this that the more water is injected, the more can be recovered. Therefore, the membrane humidification process does not affect the amount of water that can be sent to the evaporative cooler. If the absolute humidity in saturated conditions is greater than the total mass of water at the outlet, all the water would be in the vapor state. If it were less, the water would be in both liquid and vapor state. The mass of water in the liquid state can be calculated as:

$$\frac{m_{(H_2O)l,FCout}}{m_{H_2}} = \frac{m_{H_2O,FCout}}{m_{H_2}} - \frac{m_{(H_2O)v,FCout}}{m_{H_2}} \left[\frac{kg_{H_2O}}{kg_{H_2}}\right] \tag{2.23}$$

2.6. Exhaust gas cooling

A solution to increase the amount of liquid water available at the exhaust is cooling down the exhaust gas. The dry mixture does not change during cooling, therefore, the mass flow rate and molar mass of the dry mixture remain unchanged in the exhaust pipe. The calculation of the recoverable quantity of liquid water $m_{(H_2O)l,cool}$ per mass unit of

reacted hydrogen at the post-cooling temperature T_{cool} is provided in the Appendix C.

2.7. Hydrogen bus consumption evaluation

The results are presented in terms of mass unit of hydrogen consumed by the bus, ensuring the independence of the results from the precise fuel consumption of the vehicle. However, for some results, it is useful to display them over time. For this reason, it is necessary to consider a typical fuel consumption for the chosen user, specifically, an urban PEM fuel cell bus powered by hydrogen. The specific consumption of the considered vehicle can be evaluated as $9kg_{H_2}/100km$ [14]. The hydrogen density at atmospheric pressure ($0.1013MPa$) and at $0^{\circ}C$ is $0.08995kg/Nm^3$ [15], while the higher heating value (HHV_{H_2}) under the same conditions is $3.54kWh/Nm^3$ [21]. It is then possible to calculate the HHV_{H_2} per mass unit of hydrogen using the formula:

$$HHV_{H_2} = \frac{HHV_{H_2}}{\rho_{H_2}} = \frac{3.54}{0.08995} = 39.3552\left[\frac{kWh}{kg}\right] \tag{2.24}$$

The energy efficiency of the vehicle η_e can be assumed as: 62% [19]. The energy that can be exploited for the powertrain is therefore in the order of $0.62 \bullet 39.3552 = 24.4kWh/kg_{H_2}$, which means an energy consumption of $2.2kWh/km$, assuming a specific hydrogen consumption of $9kg_{H_2}/100km$. This value is in line with typical energy consumption values for rapid transit buses, shuttle buses, and regional buses, while it is slightly lower for city buses, which usually range between 2.4 and $4.6kWh/km$ for electric bus service [31]. For this reason, considering a fuel consumption of $9kg_{H_2}/100km$ can be regarded as a precautionary assumption concerning the amount of water available at the cathode outlet. City buses operate at low speeds, usually ranging between 8 and $12km/h$ (mainly due to traffic) [31]. Considering an average speed of $10km/h$ and hydrogen consumption of $9kg_{H_2}/100km$, this can be indicated in terms of time, becoming $0.9kg_{H_2}/h$.

2.8. M−cycle performance

For this study, we considered an off-the-shelf evaporative cooling system, dimensioned to match the size of the bus. In internal combustion engine buses, the power capacity for cooling typically falls within the range of $25kW$. For electric buses, or in the case of hydrogen-powered buses, the required thermal comfort for passengers remains similar [29,3]. Specifically, the goal for summer thermal comfort is to maintain a cabin temperature between 23 and $27^{\circ}C$ [31]. To meet these requirements, the bus was equipped with two Climate Wizard CW-*H*10 Indirect Evaporative Coolers [32]. The water demand of the cooling system is then compared to the water produced by the fuel cell. The performance evaluation of the CW-*H*10 system relies on the utilization of a tool provided by Seeley International. This tool enables the determination of the volumetric flow rate and temperature of the air as it exits the dry channel (and enters the bus cabin). This determination is based on the temperature and humidity conditions at the entrance of the heat exchanger. Knowing the temperature and volumetric flow rate supplied to the environment to be cooled, the subsequent calculations were carried out to evaluate the cooling capacity of an M−cycle for cooling a passenger compartment with a set point temperature. The ratio r_V between the volume flow rate supplied to the environment to be cooled $\dot{V}_{do}$ and the volume flow rate at the inlet of the M−cycle $\dot{V}_{di}$ is a specification of the chosen cooling system. The same ratio referring to the mass flow rates r_m can be calculated knowing the thermo-hygrometric conditions. The calculations are provided in the Appendix D.

The global mass and energy balances are shown in Fig. 2. The M−cycle heat exchanger is considered adiabatic to the ambient. It features an inlet for moist air and an inlet for liquid water. There are two outlets, both for moist air: one for the dry channel and one for the wet channel. The air exiting the dry channel is the supply flow, which enters the bus cabin. The cabin also has a moist air outlet for the mass balance. Additionally, the cabin experiences thermal energy input from external air, solar radiation and internal metabolic sources. For the fuel cell, the ambient air entering the cathode is humidified using an adiabatic humidifier. At the outlet, the mixture of inert gases and water enters a heat exchanger, where it is cooled. The liquid water is recovered and reused for the humidifier upstream of the cathode and for the evaporative cooler for the cabin.

The mass balance of the mixture of dry gases, considering the ratio between the mass flow rates calculated with the hypothesis of perfect mixing, can be written as:

$$\dot{m}_{da,wo} = \dot{m}_{da,di} - r_m\dot{m}_{da,di} = (1 - r_m)\dot{m}_{da,di}\left[\frac{kg_{da}}{s}\right] \tag{2.25}$$

The mass balance for water can be written as:

$$\dot{m}_{(H_2O)v,di} + \dot{m}_{(H_2O)l} = r_m\dot{m}_{(H_2O)v,di} + \dot{m}_{(H_2O)v,wo}\left[\frac{kg_{H_2O}}{s}\right] \tag{2.26}$$

from which the water consumption of the machine can be obtained.

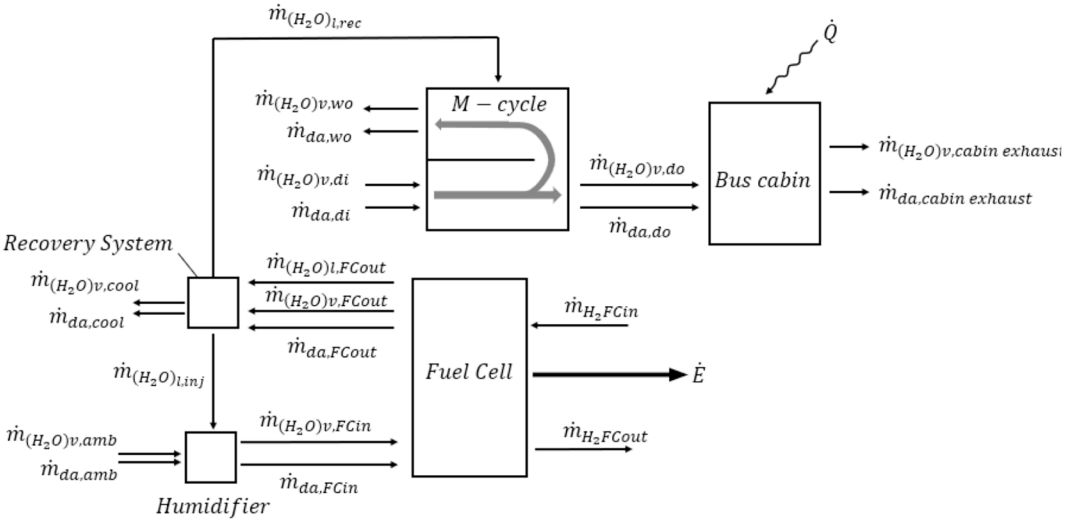

Fig. 2. Scheme for global mass and energy balances.

$$\dot{m}_{(H_2O)l} = (r_m - 1)\dot{m}_{(H_2O)v,di} + \dot{m}_{(H_2O)v,wo}\left[\frac{kg_{H_2O}}{s}\right] \tag{2.27}$$

To calculate the water consumed, however, it is necessary to know the humidity of the air flow at the wet channel outlet. Without this data it is possible to give a first estimate of around 90 % [36]. Therefore, by imposing the relative humidity at the outlet of the wet channel φ_{wo}, the relation for the absolute humidity in this condition can be written.

$$\frac{\dot{m}_{(H_2O)v,wo}}{\dot{m}_{da,wo}} = \frac{M_{H_2O}}{M_{da}} \frac{\varphi_{wo} p_{v,sat}(T_{wo})}{p_{amb} - \varphi_{wo} p_{v,sat}(T_{wo})}\left[\frac{kg_{H_2O}}{kg_{da}}\right] \tag{2.28}$$

from which we obtain the relation for the mass flow rate of water vapor at the wet channel outlet:

$$\dot{m}_{(H_2O)v,wo} = \frac{\dot{m}_{(H_2O)v,wo}}{\dot{m}_{da,wo}}\dot{m}_{da,wo} = \frac{\dot{m}_{(H_2O)v,wo}}{\dot{m}_{da,wo}}(1 - r_m)\dot{m}_{da,di}\left[\frac{kg_{H_2O}}{s}\right] \tag{2.29}$$

Finally, the global energy balance, assuming the exchanger is adiabatic with respect to the external environment, is written as:

$$\dot{m}_{da,di}c_{p,da}T_{di} + \dot{m}_{(H_2O)v,di}\left(h_{lv} + c_{p,(H_2O)v}T_{di}\right) + \dot{m}_{(H_2O)l}c_l T_l = \dot{m}_{da,do}c_{p,da}T_{do} + \dot{m}_{(H_2O)v,do}\left(h_{lv} + c_{p,(H_2O)v}T_{do}\right) + \dot{m}_{da,wo}c_{p,da}T_{wo} + \dot{m}_{(H_2O)v,wo}\left(h_{lv} + c_{p,(H_2O)v}T_{wo}\right)[W] \tag{2.30}$$

Within the global energy balance equation, the mass flow rate of water vapor at the wet channel outlet is given by equation 2.29 and, from this value, the mass flow rate of liquid water consumed can also be calculated via 2.27. The temperature of the injected liquid water was considered equal to the ambient temperature and therefore equal to the inlet temperature T_{di}. After making this hypothesis, it is possible to solve the system numerically, obtaining the outlet temperature of the wet channel and the water consumed. Finally, by setting a target temperature for the room to be cooled (in this case the bus cabin), the cooling capacity of the M−cycle can be calculated using the considered heat and mass exchanger model. This allows for determining how much heat can be dissipated based on the internal environment conditions. A quick estimation of the cooling capacity can be calculated through the equation:

$$CC = \dot{m}_{do}c_p(T_{cabin} - T_{do})[W] \tag{2.31}$$

To verify the reliability of the tool used, a dew point effectiveness map was calculated to compare the results obtained with those in the literature. To calculate the dew point effectiveness, the formula 2.32 was used. It divides the difference in dry bulb temperature between the inlet and outlet of the dry channel by the difference between the inlet dry bulb temperature and the dew point temperature of the inlet air.

$$\varepsilon_{DP} = \frac{T_{di} - T_{do}}{T_{di} - T_{di,DP}} \tag{2.32}$$

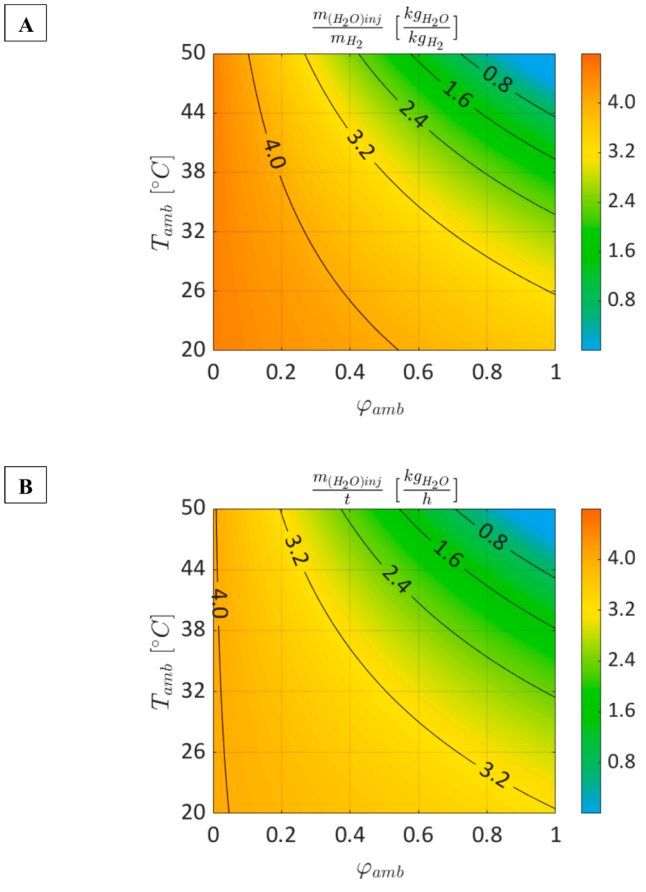

Fig. 3. Water mass per hydrogen mass unit (A) and hourly water mass flow rate (B) injected before the fuel cell to reach 80 % relative humidity at 60 °C and 1.5 bar.

3. Results

In a PEM fuel cell, it is essential to keep the membrane constantly humidified to ensure optimal performance. To achieve this, the air is humidified before entering the cathode side of the cell until the desired relative humidity is reached. Fig. 3 shows the results of calculating the amount of water required to be injected into the cathode air stream based on the thermo-hygrometric conditions of the air upstream of the humidifier. The conditions imposed at the cathode inlet of the fuel cell are a relative humidity of 80% at 60°C. Graph A shows the water mass to be injected compared to the mass of hydrogen reacted in the electrochemical cell. Graph B shows the hourly mass flow rate to be injected with regards to the analyzed case study, thus considering a fuel consumption of $9kg_{H_2}/100km$. From the graphs, as expected, it can be observed that as relative humidity decreases and temperature increases, the amount of water needed to reach the set conditions increases. This is because moving to higher temperatures or lower relative humidity reduces the absolute humidity, moving away from the required value.

As illustrated, it becomes evident that the amount of water required to achieve an air flow at 60°C with 80% humidity is not negligible. Under external ambient conditions with humidity between 30% and 60% and temperatures between 25 °C and 35°C, the water to be injected into the flow ranges from 3.2 to 4 kg per kilogram of hydrogen involved in the electrochemical reaction. This corresponds to 2.8 to 3.7 kg of water per hour for the considered case study. For this reason, in a fuel cell vehicle, implementing a system to recover the waste water produced by the cell can be advantageous in reducing the need for frequent refills of distilled water. The current alternative is to discharge the produced water into the atmosphere. Fig. 4 shows a map of the cooling capacity obtained with the Seeley tool for the M−cycle CW-H10 model. The map shows the cooling capacity of the evaporative cooling system as the inlet temperature and humidity conditions vary. The temperature of the air supplied to the environment to be cooled and the volumetric flow rate processed are parameters provided by the tool. The temperature set-

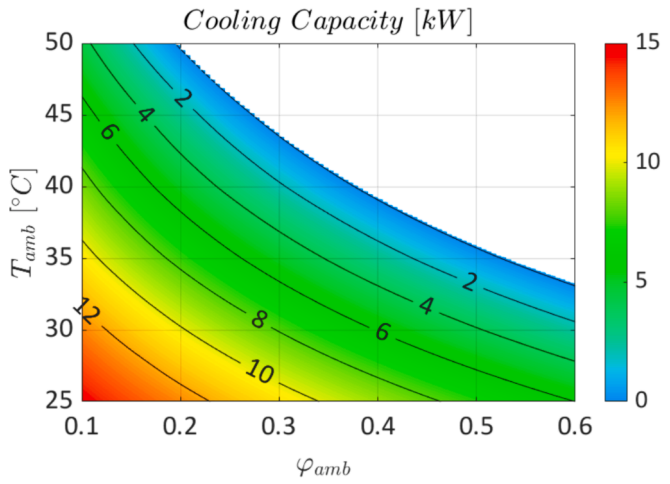

Fig. 4. CW-*H*10 M−cycle cooling capacity with cabin set-point temperature at 26 °C.

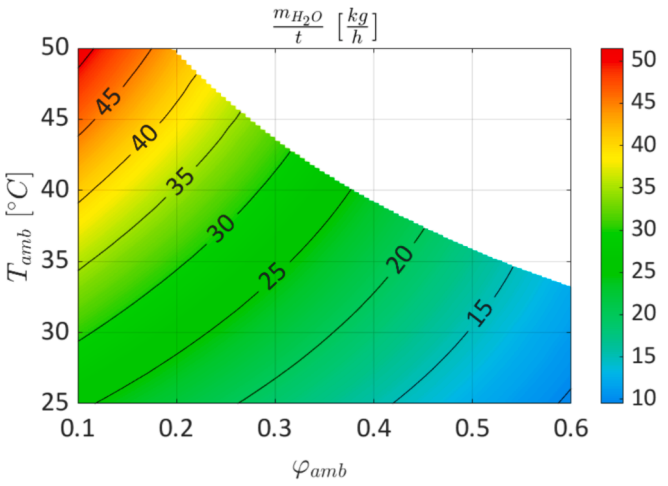

Fig. 6. CW-*H*10 M−cycle water consumption map.

point for the conditioned passenger compartment is 26°*C*.

The upper limit curve represents the cooling capacity of 0*kW*. It identifies the ambient conditions under which the outlet temperature of the CW-*H*10 matches the cabin set-point temperature, which is 26°*C* in this specific case. Beyond that line, the temperature of the air at the outlet of the evaporative cooler exceeds the set-point temperature. It is possible to observe that, under conditions such as 30°*C* ambient temperature and 30% relative humidity, a system composed of two evaporative coolers can provide 16*kW* of cooling capacity. Under these conditions, the system operates with a COP of more than 5, considering that the nominal power of each CW-*H*10 is 1.4*kW*. To obtain the same cooling capacity with a standard vapor compression cooling system with a COP of 2.5 would require higher fuel consumption and reduce the driving range. Using the results obtained with the Seeley tool, the dew point effectiveness was calculated through the equation 2.32 and is reported in Fig. 5.

From the dew point effectiveness chart for the considered Seeley system, values between 59% and 83% are calculated in the temperature range of 25°*C* to 35°*C* and relative humidity between 30% and 60%. At the inlet, for the same temperature, a decrease in relative humidity also causes a decrease in dew point effectiveness. This result, however, does not indicate a decrease in coefficient of performance of the system. This is because the difference between the inlet dry bulb temperature and the associated dew point temperature increases as the humidity of the flow decreases. The values obtained are consistent with those reported in the literature for experimental tests using an M−cycle in counterflow configuration with a channel length compatible with the CW-*H*10 machine [49,50]. Concerning the internal heat gain of the bus cabin, the metabolic heat rate released by the passengers can be estimated at 108*W*/*person* for seated passengers and 126*W*/*person* for standing passengers [9]. Hence, for a bus with 50 passengers, the overall power can be estimated to be in the order of 6*kW*. At high temperatures, the additional power that needs to be removed from the bus cabin due to solar flux can be in the order of 3-4*kW* [31]. Under these conditions, there is room for an additional 6*kW* to be removed from the cabin. Fig. 6 shows the hourly water consumption of a M−cycle CW-*H*10 system, depending on the ambient conditions of temperature and humidity.. The flow rate of water consumed is calculated based on the scheme in Fig. 2. The volume ratio between the flow rates at the outlet of the dry channel and at the inlet of the system is $r_V = 55\%$.

The water consumed needs to be multiplied by the number of installed coolers (two in this case). To obtain 16*kW* of cooling capacity with two CW-*H*10 coolers at 30°*C* ambient temperature and 30% relative humidity it is necessary to vaporize 44*kg* of water every hour. In Fig. 7, the water that can be recovered in function of oxygen excess ratio utilized and the fuel cell operating pressure is depicted. The curves illustrate trends corresponding to a hypothetical weather condition with

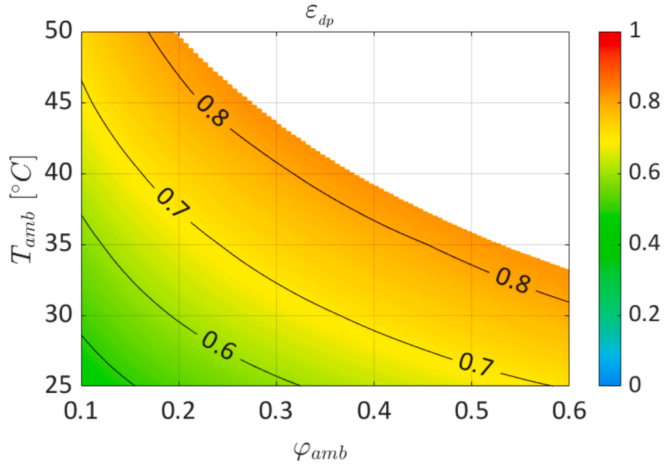

Fig. 5. CW-*H*10 dew point effectiveness under various ambient temperatures and relative humidities.

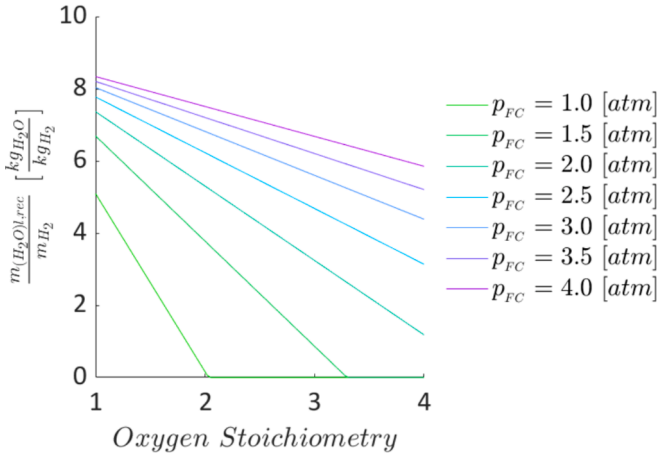

Fig. 7. Recovered liquid water at the outlet of the fuel cell in different conditions of air excess ratio and operative pressure. Calculation made at 60 °C fuel cell temperature, 30 °C ambient temperature and 30 % ambient relative humidity.

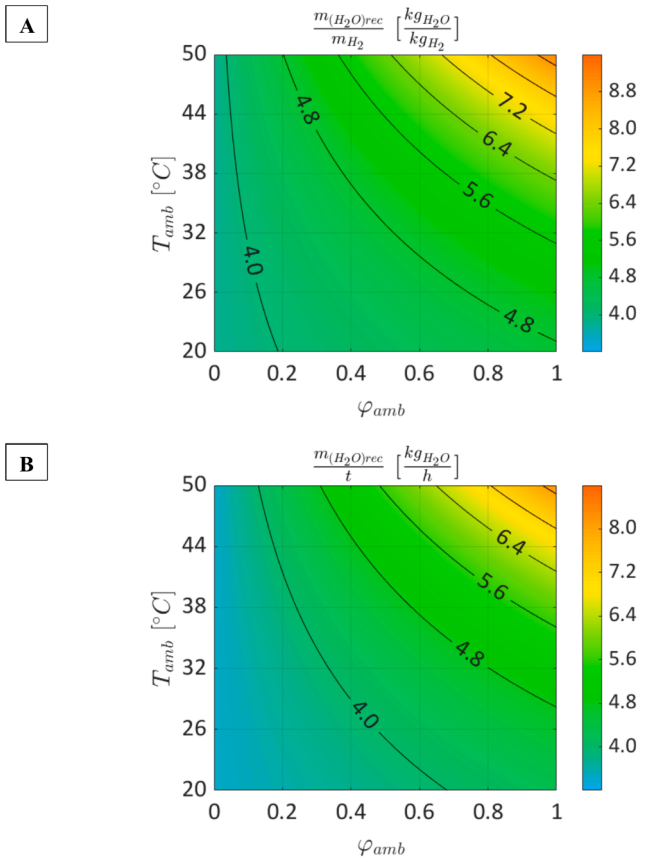

Fig. 8. Recovered water mass per hydrogen mass unit (A) and hourly recovered water mass flow rate (B) at 60 °C and 1.5 bar.

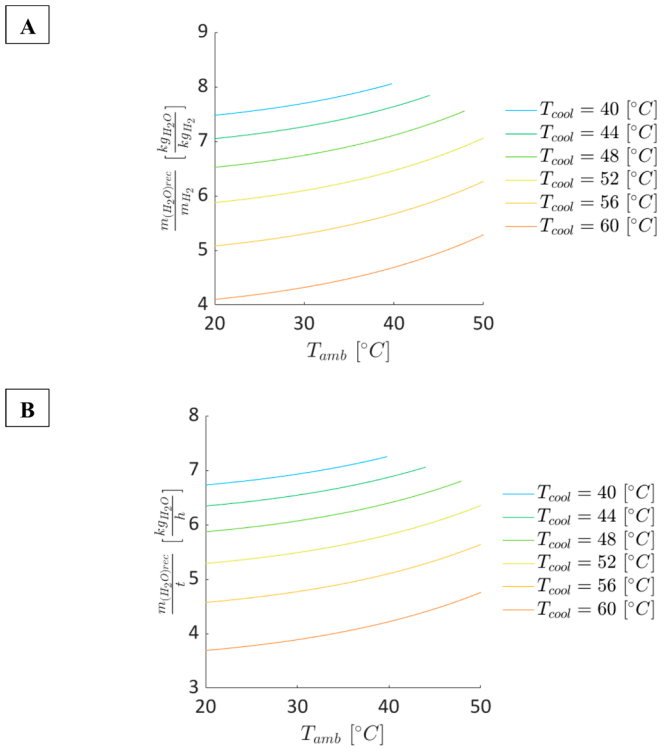

Fig. 9. Recovered liquid water mass per hydrogen mass unit (A) and hourly recovered liquid water mass flow rate (B) at different exhaust cooling temperatures, at 30% ambient relative humidity.

a temperature of 30°C and relative humidity of 30%, and the fuel cell exhaust temperature of 60°C.

As can be seen from the previous picture, increasing the operating pressure also increases the liquid water availability, while higher excess ratios reduce the liquid water availability. However, the following results (from now on) are displayed considering an operating pressure of 1.5bar and an oxygen excess ratio of 1.8, values considered optimal for fuel cell operation [1,8,33]. Under these conditions and with $T_{amb} =$ 30°C and $\varphi = 30\%$, approximately 4 kg of liquid water can be recovered for every kg of hydrogen reacted. Fig. 8 shows the amount of water that can be recovered as a function of reacted hydrogen and time. The calculation considers an outlet temperature of 60°C, representing the amount of liquid water at that temperature. The results are presented under different thermo-hygrometric ambient conditions.

Considering that for typical intense weather conditions about 40-45kg of water are needed every hour as depicted in Fig. 6, the water recovered from the hydrogen fuel cell is able to provide almost 10% of the demand. Cooling down the exhaust gas of the fuel cell is a possible solution to increase this share. Fig. 9 investigates the amount of water that can be recovered, assuming different exhaust temperatures. The curves range from 60°C down to 40°C. These curves are plotted as a function of ambient dry-bulb temperature, considering a relative humidity of 30%. The amount of water is shown per kilogram of reacted hydrogen (Graph A) and per hour (considering 0.9kg/h, Graph B). The curves are plotted only for points where the ambient temperature is lower than the exhaust temperature.

Cooling the exhaust gas down to 40°C reveals the potential to supply up to 20% of the water required by the evaporative cooling system, even under challenging hot weather conditions, leveraging the water produced by the hydrogen reaction. Hence, during the spring and autumn months, the system can approach self-sufficiency, eliminating the need for refilling distilled water. It's worth emphasizing that the term 'recovered water' refers to the quantity available for sending to the evaporative coolers, subtracted from the water needed for inlet injection to humidify the polymer membrane.

4. Conclusions

This work explores the feasibility of supplying the water discharged from a PEM fuel cell that powers an urban bus to an indirect evaporative cooling system (Maisotsenko cycle) used for conditioning the cabin. The cooling capacity of a commercial indirect evaporative cooler was estimated using the manufacturer's tool, and the results were compared to water production from the hydrogen fuel cell. Considering a set-point of 26°C in the cabin, two CW-H10 coolers can provide a cooling capacity of 16kW under an ambient temperature of 30°C and 30% relative humidity. The results show that the performance of an M−cycle can be compatible with the maximum cooling capacity demand of an urban bus. The fuel cell was modeled considering an average power request by the urban bus, corresponding to 0.9kg_{H_2}/h. Even in intense weather conditions, the fuel cell is able to provide 10 % to 20 % of the water necessary for the operation of the M−cycle, corresponding to 4 to 8kg of water recovered. To further increase the amount of recovered water it is possible to cool the fuel cell exhaust gas or operate the fuel cell at higher pressure. Having a system capable of recovering water from the fuel cell outlet is also useful for properly humidifying the membrane at the inlet without the constant need of water supply. The proposed solution boasts several advantages. Not only is the bus powered potentially without the emission of pollutants and greenhouse gases, but also the recovered water serves a dual purpose: supporting both the fuel cell and the evaporative cooling system. The latter, characterized by a remarkably high coefficient of performance, stands as an energy-efficient solution. The advantages of the indirect evaporative cooling system and hydrogen fuel cells are enhanced through their synergistic implementation. Potential areas of future interest could include an experimental application

of an indirect evaporative cooling system on an urban bus and the economic assessment of the proposed solution, comparing it to other configurations such as a traditional compressed vapor cycle operating on a hydrogen bus or an electric bus.

Declaration of Generative AI and AI-assisted technologies in the writing process

During the preparation of this work the authors used ChatGPT-3.5 in order to improve language and readability. After using this tool/service, the authors reviewed and edited the content as needed and take full responsibility for the content of the publication.

Declaration of competing interest

The authors declare that they have no known competing financial interests or personal relationships that could have appeared to influence the work reported in this paper.

Data availability

Data will be made available on request.

Acknowledgment

Funder: Project funded under the National Recovery and Resilience Plan (NRRP), Mission 4 Component 2 Investment 1.5 - Call for tender No. 3277 of 30/12/2021 of Italian Ministry of University and Research funded by the European Union – NextGenerationEU. Award Number: Project code ECS00000033, Concession Decree No. 1052 of 23/06/2022 adopted by the Italian Ministry of University and Research, CUP D93C22000460001, "Ecosystem for Sustainable Transition in Emilia-Romagna" (Ecosister), Spoke 4.

This research is also supported by Decreto Ministeriale n. 1062 del 10-08-2021, Programma Operativo Nazionale (PON) 2014-2020 "Ricerca e Innovazione" 2014-2020 - Asse IV "Istruzione e ricerca per il recupero" – Azione IV.6 – "Contratti di ricerca su tematiche Green" finalizzate al sostegno a contratti di ricerca a tempo determinato di tipologia A), di cui alla legge 30 dicembre 2010, n. 240, Art. 24, comma 3 e relativi allegati; Progetto di ricerca sulla tematica "Green" presentato dal Dipartimento di Ingegneria "Enzo Ferrari" dal titolo "FO.R.M.A. - FOnti Rinnovabili nel Mondo Agricolo".

The authors would like to thank Seeley International and Italkero SRL for the information provided.

Appendix A. Fuel cell reactions

The electrochemical reaction that takes place inside a hydrogen fuel cell is:

$$2H_2 + O_2 = 2H_2O \tag{A.1}$$

From the stoichiometry of the reaction, it is obtained that the ratios of moles of oxygen or water to hydrogen results:

$$\frac{n_{O_2,req}}{n_{H_2}} = \frac{1}{2}\left[\frac{mol_{O_2}}{mol_{H_2}}\right] \tag{A.2}$$

$$\frac{n_{H_2O,prod}}{n_{H_2}} = \frac{1}{1}\left[\frac{mol_{O_2}}{mol_{H_2}}\right] \tag{A.3}$$

From these relationships, by knowing the molar mass values of the substances involved, the mass of oxygen required $m_{O_2,req}$ and the mass of produced water $m_{H_2O,prod}$ are obtained in relation to the mass of reacted hydrogen m_{H_2}.

$$\frac{m_{O_2,req}}{m_{H_2}} = \frac{n_{O_2,req}}{n_{H_2}}\frac{M_{O_2}}{M_{H_2}} = 7.936\left[\frac{kg_{O_2}}{kg_{H_2}}\right] \tag{A.4}$$

$$\frac{m_{H_2O,prod}}{m_{H_2}} = \frac{n_{H_2O,prod}}{n_{H_2}}\frac{M_{H_2O}}{M_{H_2}} = 8.936\left[\frac{kg_{O_2}}{kg_{H_2}}\right] \tag{A.5}$$

Appendix B. Inlet humidity

The saturation pressure at the air flow ambient temperature T_{amb} can be estimated from the following relationship [34]:

$$p_{(H_2O)v,sat,amb} = 610.5e^{\frac{17.269T_{amb}}{237.3+T_{amb}}}[Pa] \tag{B.1}$$

Starting from the knowledge of the relative humidity of the ambient φ_{amb}, vapor pressure can be obtained:

$$p_{(H_2O)v,amb} = \varphi_{amb}p_{(H_2O)v,sat,amb}[Pa] \tag{B.2}$$

Knowing the atmospheric pressure is possible to derive the partial pressure of the dry air:

$$p_{da,amb} = p_{amb} - p_{(H_2O)v,amb}[Pa] \tag{B.3}$$

With these parameters it is possible to calculate the absolute humidity of the air.

By definition of absolute humidity:

$$\frac{m_{(H_2O)v,amb}}{m_{da,amb}} = \frac{M_{H_2O}}{M_{da,amb}} \frac{p_{(H_2O)v,amb}}{p_{da,amb}} \left[\frac{kg_{H_2O}}{kg_{da}}\right] \tag{B.4}$$

Considering the ratio obtained with the equation 2.4 the mass of incoming water vapor is calculated with respect to the hydrogen mass unit:

$$\frac{m_{(H_2O)v,amb}}{m_{H_2}} = \frac{m_{(H_2O)v,amb}}{m_{da,amb}} \frac{m_{da,amb}}{m_{H_2}} \left[\frac{kg_{H_2O}}{kg_{H_2}}\right] \tag{B.5}$$

Appendix C. Exhaust gas cooling

A solution to increase the amount of liquid water available at the exhaust is cooling down the exhaust gas. The dry mixture does not change during cooling, therefore, the mass flow rate and molar mass of the dry mixture remain unchanged in the exhaust pipe. The absolute saturation humidity at the post-cooling temperature T_{cool} can be calculated as:

$$\frac{m_{(H_2O)v,cool}}{m_{da,out}} = \frac{m_{(H_2O)v,sat,cool}}{m_{da,out}} = \frac{M_{H_2O}}{M_{da,out}} \frac{p_{(H_2O)v,sat}(T_{cool})}{p_{cool} - p_{(H_2O)v,sat}(T_{cool})} \left[\frac{kg_{H_2O}}{kg_{da}}\right] \tag{C.1}$$

And knowing the mass of dry gases at the exhaust per mass unit of hydrogen from equation 2.20 is possible obtain the mass of vapor per mass unit of hydrogen:

$$\frac{m_{(H_2O)v,cool}}{m_{H_2}} = \frac{m_{(H_2O)v,cool}}{m_{da,out}} \frac{m_{da,out}}{m_{H_2}} \left[\frac{kg_{H_2O}}{kg_{H_2}}\right] \tag{C.2}$$

The quantity of liquid water is determined by the difference between the total mass of water in the outlet pipe and the mass of saturated vapor downstream of the cooling process.

$$\frac{m_{(H_2O)l,cool}}{m_{H_2}} = \frac{m_{H_2O,FCout}}{m_{H_2}} - \frac{m_{(H_2O)v,cool}}{m_{H_2}} \left[\frac{kg_{H_2O}}{kg_{H_2}}\right] \tag{C.3}$$

Appendix D. M−cycle mass ratio

The partial mass flow rate of dry air and water vapor are calculated starting from the volume flow rate of the mixture with the perfect gas relation:

$$\dot{m}_i = \frac{p_i \dot{V} M_i}{RT} \left[\frac{kg_i}{s}\right] \tag{D.1}$$

From these values the total mass flow rate of the mixture can be found. The density of the mixture is:

$$\rho = \frac{\dot{m}}{\dot{V}} = \frac{\dot{m}_{da} + \dot{m}_{(H_2O)v}}{\dot{V}} = \frac{1}{\dot{V}} \frac{\dot{V}}{RT} \left(p_{da} M_{da} + p_{(H_2O)v} M_{H_2O}\right)$$

$$\rho = \frac{p_{da} M_{da} + p_{(H_2O)v} M_{H_2O}}{RT} = \frac{\left[p - \varphi p_{v,sat}(T)\right] M_{da} + \varphi p_{v,sat}(T) M_{H_2O}}{RT} \left[\frac{kg}{m^3}\right] \tag{D.2}$$

Knowing the volume flow rate of the mixture supplied to the environment to be cooled $\dot{V}_{do}$, the mass flow rate can be evaluated at the exit of the dry channel.

$$\dot{m}_{do} = \rho_{do} \dot{V}_{do} = \frac{\left[p_{do} - \varphi_{do} p_{v,sat}(T_{do})\right] M_{da} + \varphi_{do} p_{v,sat}(T_{do}) M_{H_2O}}{RT_{do}} \dot{V}_{do} \left[\frac{kg}{s}\right] \tag{D.3}$$

The relative humidity at the outlet of the dry channel of the M−cycle φ_{do} is calculated considering the dry channel outlet temperature and the dry channel inlet absolute humidity, because for the entire length of this channel, there is no variation of the absolute humidity of the flow.

$$\varphi_{do} = \frac{p_{(H_2O)v,do}}{p_{(H_2O)v,sat}(T_{do})} = \frac{\frac{\dot{m}_{(H_2O)v,amb}}{\dot{m}_{da,amb}} \frac{p_{do}}{p_{(H_2O)v,sat}(T_{do})}}{\frac{\dot{m}_{(H_2O)v,amb}}{\dot{m}_{da,amb}} + \frac{M_{H_2O}}{M_{da}}} \tag{D.4}$$

Considering the ratio r_V between the volume flow rate supplied to the environment to be cooled and the volume flow rate at the inlet of the M−cycle:

$$r_V = \frac{\dot{V}_{do}}{\dot{V}_{di}} \tag{D.5}$$

and knowing the conditions at these two locations, the same ratio referring to the mass flow rates r_m can be calculated. The density of the mixture at the inlet of the machine is again calculated with the relation D.2 referring to the inlet conditions:

$$r_m = \frac{\dot{m}_{do}}{\dot{m}_{di}} = \frac{\rho_{do}\dot{V}_{do}}{\rho_{di}\dot{V}_{di}} = \frac{\rho_{do}}{\rho_{di}} r_V \tag{D.6}$$

References

[1] A. Akroot, Ö. Ekici, M. Köksal, Process modeling of an automotive pem fuel cell system, Int. J. Green Energy 16 (10) (2019) 778–788, https://doi.org/10.1080/15435075.2019.1641105.

[2] A.-M. Cormos, I. Dumbrava, C.-C. Cormos, Evaluation of techno-economic performance for decarbonized hydrogen and power generation based on glycerol thermo-chemical looping cycles, Appl. Therm. Eng. 179 (2020) 115728, https://doi.org/10.1016/j.applthermaleng.2020.115728.

[3] D. Göhlich, T.-A. Fay, D. Jefferies, E. Lauth, A. Kunith, X. Zhang, Design of urban electric bus systems, Design Sci. 4 (2018) e15.

[4] S. Anisimov, D. Pandelidis, Theoretical study of the basic cycles for indirect evaporative air cooling, Int. J. Heat Mass Transf. 84 (2015) 974–989, https://doi.org/10.1016/j.ijheatmasstransfer.2015.01.087.

[5] X. Cui, K.J. Chua, W.M. Yang, K.C. Ng, K. Thu, V.T. Nguyen, Studying the performance of an improved dew-point evaporative design for cooling application, Appl. Therm. Eng. 63 (2) (2014) 624–633, https://doi.org/10.1016/j.applthermaleng.2013.11.070.

[6] V. Malik, S. Srivastava, M.K. Bhatnagar, M. Vishnoi, Comparative study and analysis between Solid Oxide Fuel Cells (SOFC) and Proton Exchange Membrane (PEM) fuel cell–a review, Mater. Today: Proc. 47 (2021) 2270–2275, https://doi.org/10.1016/j.matpr.2021.04.203.

[7] Z. Qi, Advances on air conditioning and heat pump system in electric vehicles – a review, Renew. Sustain. Energy Rev. 38 (2014) 754–764, https://doi.org/10.1016/j.rser.2014.07.038.

[8] Y. Qin, D. Qing, M. Fan, Y. Chang, Y. Yin, Study on the operating pressure effect on the performance of a proton exchange membrane fuel cell power system, Energ. Conver. Manage. 142 (2017) 357–365, https://doi.org/10.1016/j.enconman.2017.03.035.

[9] S.H. Hong, J.M. Lee, J.W. Moon, K.H. Lee, Thermal comfort, energy and cost impacts of PMV control considering individual metabolic rate variations in residential building, Energies 11 (2018) 1767, https://doi.org/10.3390/en11071767.

[10] V. Hacker, S. Mitsushima, Fuel Cells and Hydrogen – From Fundamentals to Applied Research, Elsevier, 2018.

[11] A.L. Dicks, D.A.J. Rand, Fuel Cell Systems Explained, John Wiley & Sons Ltd., 2018.

[12] N.N. Anand, M. Raja, T. Rangaswamy, Passive liquid water recovery from fuel cell exhaust, Int. J. Recent Res. Civil Mech. Eng. (IJRRCME) 1 (1) (2014) 18–23. Available at: www.paperpublications.org.

[13] Y. Wan, Z. Huang, A. Soh, Kian Jon Chua, On the performance study of a hybrid indirect evaporative cooling and latent-heat thermal energy storage system under commercial operating conditions, Appl. Therm. Eng. 221 (2023) 119902, https://doi.org/10.1016/j.applthermaleng.2022.119902.

[14] A. Ajanovic, R. Haas, Prospects and impediments for hydrogen and fuel cell vehicles in the transport sector, Int. J. Hydrogen Energy 46 (16) (2021) 10049–10058, https://doi.org/10.1016/j.ijhydene.2020.03.122.

[15] Y.A. Çengel, J.M. Cimbala, R.H. Turner, Fundamentals of thermal-fluid sciences, Fifth edition, McGraw-Hill Education, New York, NY, 2017.

[16] M. Chorowski, M. Lepszy, K. Machaj, Z. Malecha, D. Porwisiak, P. Porwisiak, Z. Rogala, M. Stanclik, Challenges of application of green ammonia as fuel in onshore transportation, Energies 16 (13) (2023) 4898, https://doi.org/10.3390/en16134898.

[17] W.R.W. Daud, R.E. Rosli, E.H. Majlan, S.A.A. Hamid, R. Mohamed, T. Husaini, PEM fuel cell system control: a review, Renew. Energy 113 (2017) 620–638, https://doi.org/10.1016/j.renene.2017.06.027.

[18] K.G. Logan, J.D. Nelson, A. Hastings, Electric and hydrogen buses: shifting from conventionally fuelled cars in the UK, Transp. Res. Part D: Transp. Environ. 85 (2020) 102350.

[19] H. Lohse-Busch, K. Stutenberg, M. Duoba, X. Liu, A. Elgowainy, M. Wang, B. Thomas Wallner, M.C. Richard, Automotive fuel cell stack and system efficiency and fuel consumption based on vehicle testing on a chassis dynamometer at minus 18 °C to positive 35 °C temperatures, Int. J. Hydrogen Energy 45 (1) (2020) 861–872, https://doi.org/10.1016/j.ijhydene.2019.10.150.

[20] S. Mekhilef, R. Saidur, A. Safari, Comparative study of different fuel cell technologies, Renew. Sustain. Energy Rev. 16 (1) (2012) 981–989, https://doi.org/10.1016/j.rser.2011.09.020.

[21] H. Miland, Ø. Ulleberg, Testing of a small-scale stand-alone power system based on solar energy and hydrogen, Sol. Energy 86 (1) (2012) 666–680, https://doi.org/10.1016/j.solener.2008.04.013.

[23] P. Pei, M. Ouyang, Q. Lu, H. Huang, X. Li, Testing of an automotive fuel cell system, Int. J. Hydrogen Energy 29 (10) (2004) 1001–1007, https://doi.org/10.1016/j.ijhydene.2004.01.008.

[24] T. Taner, The novel and innovative design with using H2 fuel of PEM fuel cell: efficiency of thermodynamic analyze, Fuel 302 (2021) 121109, https://doi.org/10.1016/j.fuel.2021.121109.

[25] G. Trencher, A. Edianto, Drivers and barriers to the adoption of fuel cell passenger vehicles and buses in Germany, Energies 14 (4) (2021) 833, https://doi.org/10.3390/en14040833.

[26] Z. Wang, J. Yu, G. Li, C. Zhuge, A. Chen, Time for hydrogen buses? dynamic analysis of the Hong Kong bus market, Transport. Res. Part D: Transport Environ. 115 (2023), https://doi.org/10.1016/j.trd.2022.103602.

[27] N. Zacharof, O. Özener, S. Broekaert, M. Özkan, Z. Samaras, G. Fontaras, The impact of bus passenger occupancy, heating ventilation and air conditioning systems on energy consumption and CO2 emissions, Energy 272 (ISSN 0360–5442) (2023), https://doi.org/10.1016/j.energy.2023.127155, 127155.

[28] H.S. Dizaji, H. Eric Jing, L. Chen, A comprehensive review of the Maisotsenko-cycle based air conditioning systems, Energy 156 (2018) 725–749, https://doi.org/10.1016/j.energy.2018.05.086. ISSN 0360–5442,.

[29] I.-S. Suh, M. Lee, J. Kim, O. Sang Taek, J.-P. Won, Design and experimental analysis of an efficient HVAC (heating, ventilation, air-conditioning) system on an electric bus with dynamic on-road wireless charging, Energy 81 (2015) 262–273, https://doi.org/10.1016/j.energy.2014.12.038. ISSN 0360–5442,.

[30] Guangya Zhu, Tao Wen, Qunwei Wang, Xiaoyu Xu, A review of dew-point evaporative cooling: recent advances and future development, App. Energy 312 (2022), 118785, ISSN 0306-2619, doi: 10.1016/j.apenergy.2022.118785.

[31] H. Basma, C. Mansour, M. Haddad, M. Nemer, P. Stabat, Energy consumption and battery sizing for different types of electric bus service, Energy 239 (ISSN 0360–5442) (2022), https://doi.org/10.1016/j.energy.2021.122454. Part E 122454.

[32] Seeley International, Available online at: https://www.seeleyinternational.com/eu/artefact/climate-wizard-indirect-evaporative-air-conditioning-brochure/, accessed on 22 December 2023.

[33] Z. Liu, L. Li, Y. Ding, H. Deng, W. Chen, Modeling and control of an air supply system for a heavy duty PEMFC engine, Int. J. Hydrogen Energy 41 (36) (2016) 16230–16239, https://doi.org/10.1016/j.ijhydene.2016.04.213. ISSN 0360-3199.

[34] Fantucci, Stefano; Fenoglio, Elisa; Serra, Valentina; Perino, Marco; Coupled Heat And Moisture Transfer Simulations On Building Components Retrofitted With A Newly Developed Aerogel-based Coating; 16th IBPSA International Conference and Exibition tenutosi a Roma nel 2- 4/09/2029) doi: 10.26868/25222708.2019.211077.

[35] Arthur N. Cox, Allen's Astrophysical Quantities, Fourth Edition, 2002 Springer Science+Business Media New York, ISBN 978-1-4612-7037-9, DOI 10.1007/978-1-4612-1186-0.

[36] P. Xu, X. Ma, X. Zhao, K. Fancey, Experimental investigation of a super performance dew point air cooler, Appl. Energy 203 (2017) 761–777, https://doi.org/10.1016/j.apenergy.2017.06.095.

[37] Mahmood, M. H., Sultan, M., Miyazaki, T., Koyama, S., & Maisotsenko, V. S. (2016). Overview of the Maisotsenko cycle – a way towards dew point evaporative cooling, Renew. Sustain. Energy Reviews 66. Elsevier Ltd. Doi: 10.1016/j.rser.2016.08.022, pp. 537–555.

[38] H. Chen, Z. Liu, Xichen Ye, Liu Yi, Sichen Xu, Tong Zhang, Air flow and pressure optimization for air supply in proton exchange membrane fuel cell system, Energy 238 (Part C) (2022), https://doi.org/10.1016/j.energy.2021.121949, 121949.

[39] G. Leoncini, R. Mothier, B. Michel, M. Clausse, A review on challenges concerning thermal management system design for medium duty electric vehicles, Appl. Therm. Eng. 236 (Part A) (2024), https://doi.org/10.1016/j.applthermaleng.2023.121464, 121464.

[40] S. Vashisht, D. Rakshit, Recent advances and sustainable solutions in automobile air conditioning systems, J. Clean. Prod. 329 (2021) 129754, https://doi.org/10.1016/j.jclepro.2021.129754.

[41] Zhongbao Wei, Ruoyang Song, Dongxu Ji, Yanbo Wang, Fengwen Pan, Hierarchical thermal management for PEM fuel cell with machine learning approach, Appl. Therm. Eng., 236, Part B, 2024, 121544, Doi: 10.1016/j.applthermaleng.2023.121544.

[42] L. Xing, W. Xiang, R. Zhu, T. Zhengkai, Modeling and thermal management of proton exchange membrane fuel cell for fuel cell/battery hybrid automotive vehicle, Int. J. Hydrogen Energy 47 (3) (2022) 1888–1900, https://doi.org/10.1016/j.ijhydene.2021.10.146.

[43] G. Zhu, T.-T. Chow, V.S. Maisotsenko, T. Wen, Maisotsenko power cycle technologies: research, development and future needs, Appl. Therm. Eng. 223 (2023) 120023, https://doi.org/10.1016/j.applthermaleng.2023.120023.

[44] C.R. Broliato, C.R. Altafini, C.A. Costa, Development of an evaporative cooler system applied to the air conditioning of urban buses, Scientia Cum Industria 8 (1) (2020) 46–56, https://doi.org/10.18226/23185279.v8iss1p46.

[45] K. Jignesh Vaghela, Comparative evaluation of an automobile air - conditioning system using R134a and its alternative refrigerants, EnergyProcedia 109 (2017) 153–160, https://doi.org/10.1016/j.egypro.2017.03.083.

[46] K. Kant, A. Kumar, S.C. Mullick, Space conditioning using evaporative cooling for summers in Delhi, Build. Environ. 36 (1) (2001) 15–25, https://doi.org/10.1016/S0360-1323(99)00060-8.
[47] Q. Luo, C. Ou, J. Hang, Z. Luo, H. Yang, X. Yang, X. Zhang, Y. Li, X. Fan, Role of pathogen-laden expiratory droplet dispersion and natural ventilation explaining a COVID-19 outbreak in a coach bus, Build. Environ. 220 (2022), https://doi.org/10.1016/j.buildenv.2022.109160.
[48] C. Ou, S. Hu, K. Luo, H. Yang, J. Hang, P. Cheng, Z. Hai, S. Xiao, H. Qian, S. Xiao, X. Jing, Insufficient ventilation led to a probable long-range airborne transmission of SARS-CoV-2 on two buses, Build. Environ. 207 (2022), https://doi.org/10.1016/j.buildenv.2021.108414.
[49] Z. Duan, X. Zhao, C. Zhan, X. Dong, H. Chen, Energy saving potential of a counter-flow regenerative evaporative cooler for various climates of China: experiment-based evaluation, Energ. Buildings 148 (2017) 199–210, https://doi.org/10.1016/j.enbuild.2017.04.012.
[50] S. Kashyap, J. Sarkar, A. Kumar, Development and experimental analysis of a novel dual-mode counter-flow evaporative cooling device, Build. Environ. 205 (2021) 108176, https://doi.org/10.1016/j.buildenv.2021.108176.
[51] Z. Wang, J. Yu, G. Li, C. Zhuge, A. Chen, Time for hydrogen buses? Dynamic analysis of the Hong Kong bus market, Transport. Res. Part D: Transport Environ. 115 (2023), https://doi.org/10.1016/j.trd.2022.103602.